Cyclic Peptides

Deutsche Ausgabe: DOI: 10.1002/ange.201411594
Internationale Ausgabe: DOI: 10.1002/anie.201411594

Intracellular Delivery of Peptidyl Ligands by Reversible Cyclization: Discovery of a PDZ Domain Inhibitor that Rescues CFTR Activity**

*Ziqing Qian, Xiaohua Xu, Jeanine F. Amacher, Dean R. Madden, Estelle Cormet-Boyaka, and Dehua Pei**

Abstract: *A general strategy was developed for the intracellular delivery of linear peptidyl ligands through fusion to a cell-penetrating peptide and cyclization of the fusion peptides via a disulfide bond. The resulting cyclic peptides are cell permeable and have improved proteolytic stability. Once inside the cell, the disulfide bond is reduced to produce linear biologically active peptides. This strategy was applied to generate a cell-permeable peptide substrate for real-time detection of intracellular caspase activities during apoptosis and an inhibitor for the CFTR-associated ligand (CAL) PDZ domain as a potential treatment for cystic fibrosis.*

The application of peptides as drugs is limited by their proteolytic instability and poor membrane permeability. Cyclization[1] or stapling[2] of peptides greatly improves their proteolytic stability. Moreover, it was recently discovered that cyclic peptides containing certain amphipathic sequences (e.g., FΦRRRR, where Φ is L-2-naphthylalanine) efficiently enter mammalian cells through endocytosis.[3–5] Biologically active cyclic peptides can be delivered into the cytosol and nucleus of mammalian cells by incorporating into them these short sequence motifs.[3,4,6] However, in many circumstances, binding to a molecular target (e.g., PDZ[7,8] and BIR[9] domains) requires that the peptidyl ligand exist in an extended conformation (e.g., β-strand) and cyclization or stapling interferes with target binding. Herein, we report a potentially general strategy for delivering linear peptides into mammalian cells through reversible disulfide-mediated cyclization. When present in the oxidizing extracellular or endosomal environment, the peptides exist as macrocycles, the rigidified structures of which enhance their proteolytic stability and cell permeability. Upon entering the cytosol of a cell, the disulfide bond is reduced by intracellular thiols to produce linear biologically active peptides[10,11] (Figure 1).

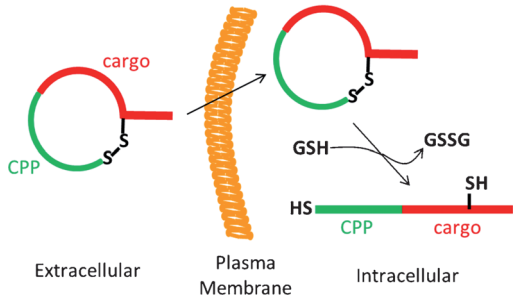

Figure 1. Scheme of the reversible cyclization strategy for delivering peptidyl cargos into mammalian cells. GSH = glutathione.

We recently reported a cyclic peptide, cyclo(FΦRRRRQ) (cFΦR$_4$), as a novel cell-penetrating peptide (CPP) that binds directly to plasma membrane phospholipids, enters cells via multiple endocytic mechanisms, and efficiently escapes from the early endosome.[3,4] With a cytosolic/nuclear delivery efficiency 4–12-fold higher than that of nonaarginine (R$_9$), Tat, and penetratin,[4,12] cFΦR$_4$ is one of the most active CPPs known to date. To test the validity of the reversible cyclization strategy, we synthesized peptide HSCH$_2$CH$_2$CO-FΦRRRRCK-NH$_2$ and cyclized it through an intramolecular disulfide bond (Table 1, peptide **1**; Figure S1 in the Supporting Information). A linear control peptide with the same sequence (Table 1, peptide **2**; Figure S1) was also synthesized by replacing the N-terminal 3-mercaptopropionyl group with a butyryl group and the C-terminal cysteine residue with 2-aminobutyric acid (Abu or U). Both peptides were labeled at the side chain of a C-terminal lysine with fluorescein isothiocyanate (FITC), and their cellular uptake was assessed by live-cell confocal microscopy and flow cytometry. HeLa cells treated with cyclic peptide **1** showed strong diffuse green fluorescence throughout the entire cell, while rhodamine-labeled dextran (dextran^{Rho}, an endocytosis marker) exhibited only punctate fluorescence in the cytoplasmic region (Figure 2a). The nearly uniform distribution of FITC fluorescence in both cytoplasmic and nuclear regions suggests that the cyclic peptide was efficiently internalized by HeLa cells and that like the parent peptide, cFΦR$_4$, it was able to efficiently escape from the endosome. By contrast, cells treated with peptide **2** showed much weaker fluorescence

[*] Dr. Z. Qian, Prof. Dr. D. Pei
Department of Chemistry and Biochemistry
The Ohio State University
484 West 12th Avenue, Columbus, OH 43210 (USA)
E-mail: pei.3@osu.edu
Dr. X. Xu, Prof. Dr. E. Cormet-Boyaka
Department of Veterinary Biosciences
The Ohio State University
1950 Coffey Road, Columbus, OH 43210 (USA)
Dr. J. F. Amacher, Prof. Dr. D. R. Madden
Department of Biochemistry, Dartmouth Medical School
7200 Vail Building, Hanover, NH 03755 (USA)

[**] This work was supported by grants from the National Institutes of Health (GM062820, CA132855, DK101451, and T32 GM008704) and Cystic Fibrosis Foundation RDP award STANTO11R0. We thank Dr. A. M. Barrios (Univ. Utah) for providing phosphocoumaryl aminopropionic acid.

Supporting information for this article is available on the WWW under http://dx.doi.org/10.1002/anie.201411594.

Table 1: Sequences of the peptides used in this work.[a]

Peptide	Sequence
1	FITC-CRRRRFWQCTRV-NH_2 (S–S)
2	$CH_3CH_2CH_2$CO-FΦRRRRUK(FITC)-NH_2
3	CH_3CO-DMUD-AMC
4	CH_2CH_2CO-RRRRΦFDMCD-AMC (S–S)
5	CH_2CH_2CO-RRRRΦFDMCD-AMC (S–S)
6	$CH_3CH_2CH_2$CO-RRRRΦFDMUD-AMC
7	CH_3CO-RRRRRRRRRDMUD-AMC
8	FITC-CRRRRFWQCTRV-OH (S–S)
9	FITC-URRRRFWQUTRV-OH
10	FITC-CRRRRFWQCTRV-NH_2 (S–S)

[a] AMC = 7-amino-4-methylcourmarin, FITC = fluorescein isothiocyanate, Φ = L-2-naphthylalanine, M = norleucine, U = 2-aminobutyric acid.

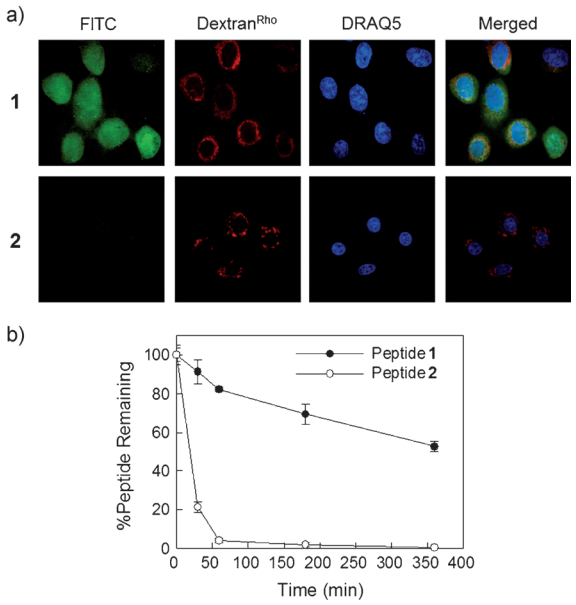

Figure 2. Comparison of the cellular uptake efficiency and proteolytic stability of disulfide-cyclized (**1**) and linear (**2**) CPPs. a) Live-cell confocal microscopy images of HeLa cells after treatment for 1 h with 5 μM FITC-labeled peptide **1** or **2**, Dextran^{Rho} (0.5 mg mL^{-1}), and nuclear staining dye DRAQ5. All images were recorded in the same Z-section. b) Plot of the percentage of remaining peptide **1** or **2** as a function of incubation time in human serum (37 °C). Data reported represent the mean ± SD from three independent experiments.

under the same conditions. Quantitation by flow cytometry gave mean fluorescence intensity (MFI) values of 27100, 5530, and 1200 for cells treated with peptides **1**, **2**, and FITC alone, respectively. We also used a hydrophilic peptide, Asp-Glu-pCAP-Leu-Ile (PCP, where pCAP is phosphocoumaryl aminopropionic acid),[4] as cargo and attached it to peptides **1** and **2** through a polyethyleneglycol linker (Figure S1 in the Supporting Information). pCAP is nonfluorescent but, upon entry into the cytosol, it undergoes rapid dephosphorylation to generate a fluorescent product, coumaryl aminopropionic acid (CAP).[13] The pCAP assay therefore provides a quantitative assessment of the cytosolic/nuclear CPP concentration.[3,4] Flow cytometry analysis of HeLa cells treated with 5 μM peptide **1**-PCP and peptide **2**-PCP gave MFI values of 3020 and 700, respectively (Figure S2). Cyclization of FΦRRRR through a disulfide bond thus has a similar effect to N-to-C cyclization and increases the cellular internalization efficiency by approximately 5-fold. Disulfide cyclization also greatly enhances the proteolytic stability of the peptide. Incubation of peptide **1** in human serum for 360 min at 37 °C resulted in 48 % degradation ($t_{1/2} \approx 6$ h), whereas under the same conditions, peptide **2** was completely degraded within 180 min ($t_{1/2} \approx 15$ min; Figure 2b).

To illustrate the utility of the reversible cyclization strategy, we applied it to deliver a caspase substrate into mammalian cells and monitor intracellular caspase activity in real time.[14] Although peptidyl coumarins have been used as caspase substrates in vitro,[15] they are not membrane permeable and are thus not suitable for in vivo applications. To generate a cell-permeable caspase substrate, we fused the caspase 3/7 substrate Ac-Asp-Nle-Abu-Asp-AMC[16] (Table 1, peptide **3**, where AMC is 7-amino-4-methylcoumarin and Nle is norleucine; Figure S3) to the CPP motif RRRRΦF (Figure 3a). The fusion peptide was cyclized by appending a 3-mercaptopropionyl group to its N terminus, replacing the Abu residue with a cysteine, and forming an intramolecular disulfide bond between the thiol groups to give peptide **4** (Table 1; Figure S3). For comparison, we synthesized an irreversibly cyclized peptide (Table 1, peptide **5**; Figure S3) through the formation of a thioether bond

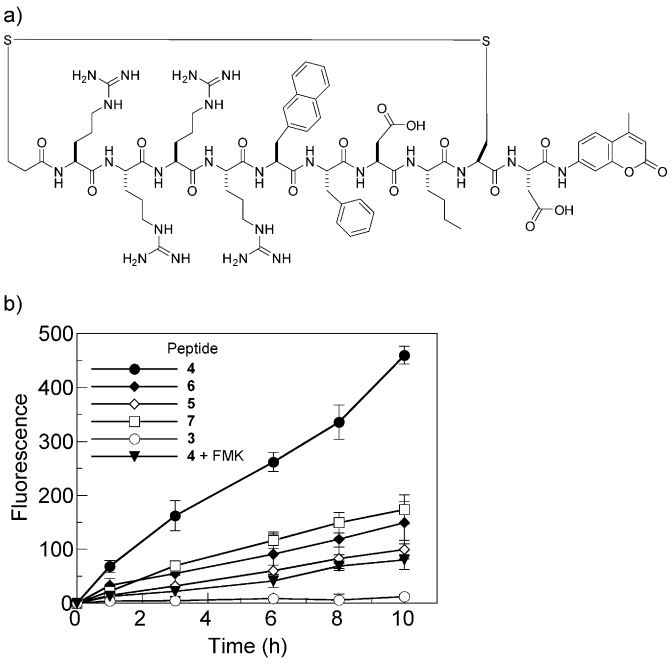

Figure 3. a) Structure of disulfide-cyclized caspase substrate **4**. b) Time-dependent release of AMC by Jurkat cells treated with peptides **3**–**7** (5 μM) in the absence and presence of caspase inhibitor FMK (100 μM). Data reported represent the mean ± SD from three independent experiments.

between an N-terminal 4-bromobutyryl moiety and the C-terminal cysteine. A linear control peptide of the same sequence was also prepared as described above (Table 1, peptide **6**; Figure S3). Finally, the caspase 3/7 substrate was conjugated to R_9 to produce a positive control peptide (Table 1, peptide **7**; Figure S3). In vitro kinetic analysis revealed that conjugation of the caspase 3/7 substrate to RRRRΦF and R_9 decreased its susceptibility to caspase cleavage relative to peptide **3** by 53% and 72%, respectively, whereas irreversible cyclization rendered the substrate completely resistant to cleavage by caspase 3 (Table S1). The enzymatic activity of caspase 3 toward peptide **4** could not be determined because the caspase assay requires reducing conditions, which would cleave the disulfide bond. Given the structural similarity between peptides **4** and **5**, we expected peptide **4** to be resistant to cleavage by caspases but to be susceptible at a similar level to peptide **6** upon reduction of the disulfide bond (Table S1).

Jurkat cells were pretreated with the kinase inhibitor staurosporin to induce caspase activity. The cells were then incubated with peptides **3**–**7** and the amount of AMC released was monitored over time (0–10 h). The measured fluorescence values were normalized to the value measured for the negative control (cells without staurosporin treatment). As expected, the impermeable caspase substrate **3** produced little fluorescence increase over the 10 h period (Figure 3b). Peptide **4** produced the fastest increase, with the fluorescence reaching 459 in 10 h, followed by the R_9-conjugated peptide **7** and the linear peptide **6**. The irreversibly cyclized peptide **5**, which is resistant to cleavage by caspase 3 in vitro, also produced AMC in a time-dependent manner, albeit at a much lower rate (fluorescence intensity of 99 after 10 h). We attribute this slow AMC release to hydrolysis by other intracellular enzymes. Consistent with this hypothesis, Jurkat cells pretreated with the pan-caspase inhibitor Z-VAD-(OMe)-CH_2F (FMK)[17] followed by peptide **4** released AMC at a rate similar to those treated with peptide **5** alone. The simplest interpretation of the above data is that both peptides **4** and **5** enter the cell interior efficiently but only peptide **4** is converted into the linear active caspase substrate inside the cell.

Many protein–protein interactions (PPIs) are mediated by protein domains binding to short peptides in their extended conformations (e.g., α-helix and β-strand).[18] For example, the PDZ domain is a globular interaction module containing 80–90 amino acids and is found in numerous proteins from diverse organisms from bacteria to man.[7,8,19] PDZ domains recognize specific sequences at the C termini of their binding partners and the bound peptide ligands adopt an extended β-strand conformation.[7,20] It was recently reported that the activity of cystic fibrosis transmembrane conductance regulator (CFTR), a chloride ion channel protein mutated in cystic fibrosis (CF) patients, is negatively regulated by CFTR-associated ligand (CAL) through its PDZ domain (CAL-PDZ).[21] Inhibition of the CFTR/CAL-PDZ interaction was shown to improve the activity of ΔF508-CFTR, the most common CF-causing mutation,[22,23] by reducing its lysosomal degradation.[21,24] Previous library screening and rational design have identified several moderately potent peptidyl inhibitors against the CAL-PDZ domain (K_D values in the high nM to low μM range).[24–27] However, these peptidyl inhibitors are membrane impermeable and thus have limited therapeutic potential.

Starting from a previously reported CAL-PDZ domain ligand, WQVTRV,[25] we designed a disulfide-cyclized peptide by adding the sequence CRRRRF to its N terminus and replacing the Val residue at the −3 position (relative to the C-terminal Val, which is designated as position 0) with a cysteine (Figure 4a; Figure S4; Table 1 peptide **8**). The tryptophan residue at the −5 position was designed to serve dual functions of PDZ binding and membrane translocation (as a replacement for L-naphthylalanine). A FITC group was added to the N terminus to facilitate affinity and cellular uptake measurements. Two structurally similar control peptides were also prepared. The linear peptide **9** contains two Abu residues instead of the Cys residues, whereas peptide **10** has an amidated C terminus, which should abolish PDZ domain binding (Figure S4).[8] Fluorescence anisotropy (FA) analysis showed that in the absence of a reducing agent, peptide **8** shows no detectable binding to the CAL-PDZ domain (Figure 4b). In the presence of 2 mM tris(carboxylethyl)phosphine, however, peptide **8** (the reduced form) bound to the CAL-PDZ domain with a K_D value of 490 ± 130 nM. As expected, peptide **10** did not bind the PDZ domain under any conditions (Figure S5). Peptide **8** was readily cell permeable; incubation of HeLa cells with peptide **8** (5 μM for 2 h) resulted in intense and diffuse fluorescence throughout the entire cell (Figure 4c). Flow cytometry showed that peptide **10** entered cells with similar efficiency as peptide **8**, whereas peptide **9** showed approximately 4-fold lower cell uptake efficiency (Figure S5). Peptide **8** showed superior serum stability compared to a control peptide in which the PDZ ligand was attached to the Gln side chain of $cF\Phi R_4$ (Figure S6, peptide **11**).

Peptide **8** was tested for its ability to rescue the chloride ion transport activity of ΔF508-CFTR. This activity was assessed by 6-methoxy-*N*-(3-sulfopropyl)-quinolinium (SPQ) assay on human bronchial epithelial CFBE41o- (CFBE) cells, which are homozygous for the ΔF508-CFTR mutation.[28] Briefly, CFBE cells were first treated with 20 μM of the small-molecule CFTR corrector VX809[29] for 24 h, which enhances the folding of mutant CFTR protein, and then incubated for 2 h with 50 μM peptide **8**. The cells were next loaded with the halide-sensitive SPQ fluorophore by using hypotonic shock, washed with sodium iodide containing fluorescence quenching buffer, and incubated with a dequenching isotonic sodium nitrate buffer. Pharmacological activation of CFTR with forskolin and genistein results in increased SPQ fluorescence, which correlates with iodide efflux. A negative control experiment in the presence of the CFTR inhibitor GlyH101 was performed to determine the amount of non-CFTR-mediated iodide efflux. A combination of VX809 and peptide **8** increased the activity of the mutant CFTR by 77% (Figure 4d). By contrast, VX809 alone, VX809 in combination with linear peptide **9**, or VX809 in combination with the C-terminally amidated peptide **10** resulted in no significant ($\leq 27\%$) increase in CFTR activity (Figure 4d; Figure S7). Treatment of CFBE cells with another

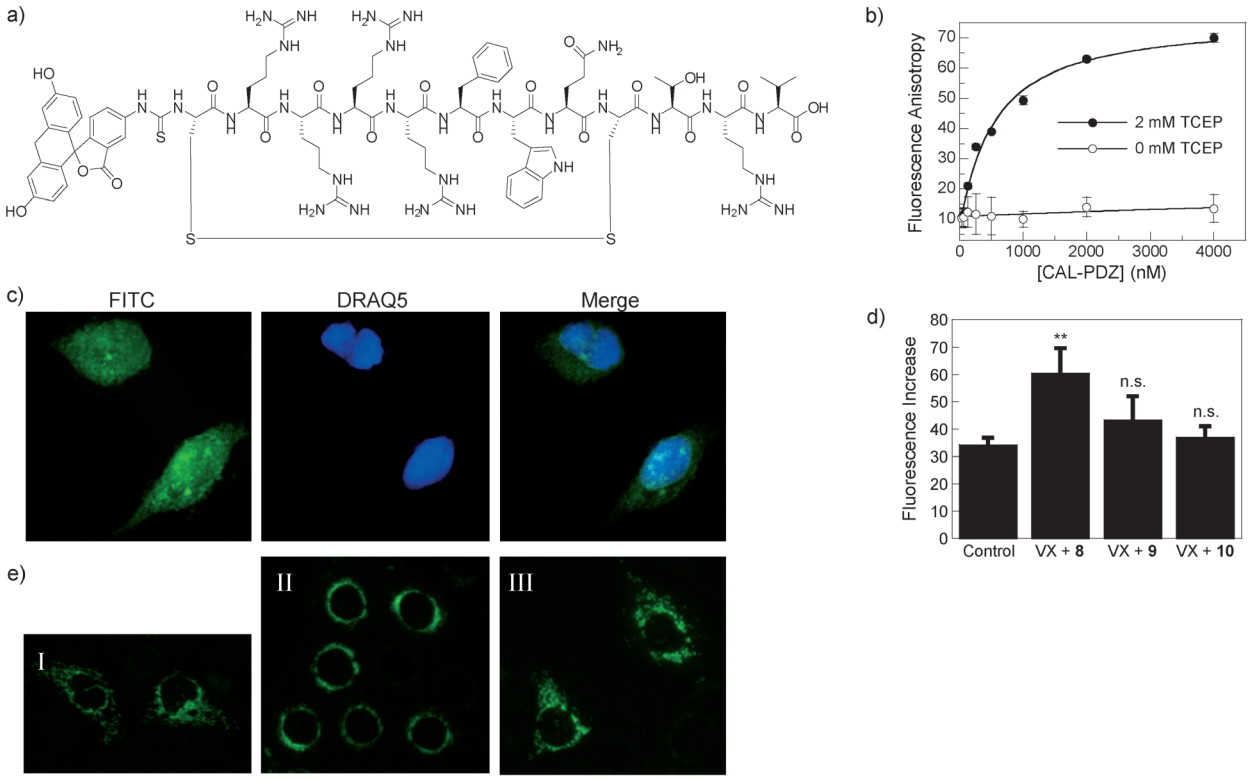

Figure 4. a) Structure of FITC-labelled peptide **8**. b) Binding of FITC-labelled peptide **8** to the CAL-PDZ domain in the presence or absence of reducing reagent as analyzed by fluorescence anisotropy. Data reported represent the mean ± SD from three independent experiments. c) Live-cell confocal microscopy images of HeLa cells treated with FITC-labelled peptide **8** (5 μM) and nuclear stain DRAQ5 in the same Z-section. d) Rescue of ΔF508-CFTR activity in CFBE cells by treatment with VX809 (20 μM) in combination with peptide **8**, **9**, or **10** (50 μM) as monitored by the SPQ assay. Fluorescence increase in the *y* axis reflects the ion channel activity of the ΔF508-CFTR protein. ** indicates $p < 0.01$ relative to the control (no VX809 or peptide) by two-tailed t-test ($n = 4$). e) Immunofluorescence staining of CFTR protein in wild-type human bronchial epithelial (16HBE) cells (I) or CFBE cells before (II) and after (III) treatment with 20 μM Corr-4a and 50 μM peptide **8**.

small-molecule corrector, Corr-4a[30] (20 μM), and 50 μM peptide **8** also improved the ion transport activity of ΔF508-CFTR, albeit less effectively (Figure S8). Immunofluorescence staining with an anti-CFTR antibody showed that while wild-type CFTR is distributed throughout the cytoplasm of bronchial epithelial (16HBE) cells, ΔF508-CFTR is localized predominantly in the perinuclear region in approximately 47% of the untreated CFBE cells or CFBE cells treated with Corr-4a only (Figure 4e; Figure S8). Treatment of the CFBE cells with booth Corr-4a and peptide **8** (but not peptide **10**) significantly increased the population of CFBE cells with wild-type-like CFTR distribution (from 53% to 67%). Taken together, our data suggest that peptide **8** inhibits the CFTR/CAL-PDZ interaction, reduces lysosome-mediated degradation of the ΔF508-CFTR protein, and further increases the ion transport activity of the mutant CFTR in the presence of small-molecule correctors.

In summary, we have demonstrated that the incorporation of short amphipathic CPP motifs coupled with disulfide-mediated cyclization provides a novel approach for the intracellular delivery of linear peptidyl cargos into mammalian cells. Cyclization of the bifunctional peptides confers both improved delivery efficiency and improved proteolytic stability, while the reversibility of the disulfide bond permits the release of functional linear peptides inside the cell.

Keywords: cell-penetrating peptides · cyclic peptides · cystic fibrosis · PDZ domains · protein–protein interactions

How to cite: *Angew. Chem. Int. Ed.* **2015**, *54*, 5874–5878
Angew. Chem. **2015**, *127*, 5972–5976

[1] L. T. Nguyen, J. K. Chau, N. A. Perry, L. de Boer, S. A. J. Zaat, H. J. Vogel, *PLoS One* **2010**, *5*, e12684.
[2] L. D. Walensky, G. H. Bird, *J. Med. Chem.* **2014**, *57*, 6275–6288.
[3] Z. Qian, T. Liu, Y. Y. Liu, R. Briesewitz, A. M. Barrios, S. M. Jhiang, D. Pei, *ACS Chem. Biol.* **2013**, *8*, 423–431.
[4] Z. Qian, J. R. LaRochelle, B. Jiang, W. Lian, R. L. Hard, N. G. Selner, R. Luechapanichkul, A. M. Barrios, D. Pei, *Biochemistry* **2014**, *53*, 4034–4046.
[5] D. Oh, S. A. Darwish, A. N. Shirazi, R. K. Tiwari, K. Parang, *ChemMedChem* **2014**, *9*, 2449–2453.
[6] W. Lian, B. Jiang, Z. Qian, D. Pei, *J. Am. Chem. Soc.* **2014**, *136*, 9830–9833.
[7] D. A. Doyle, A. Lee, J. Lewis, E. Kim, M. Sheng, R. MacKinnon, *Cell* **1996**, *85*, 1067–1076.
[8] J. H. Morais Cabral, C. Petosa, M. J. Sutcliffe, S. Raza, O. Byron, F. Poy, S. M. Marfatia, A. H. Chishti, R. C. Liddington, *Nature* **1996**, *382*, 649–652.
[9] G. Wu, J. Chai, T. L. Suber, J. W. Wu, C. Du, X. Wang, Y. Shi, *Nature* **2000**, *408*, 1008–1012.
[10] L. Cascales, S. T. Henriques, M. C. Kerr, Y.-H. Huang, M. J. Sweet, N. L. Daly, D. J. Craik, *J. Biol. Chem.* **2011**, *286*, 36932–36943.

[11] D. Jha, R. Mishra, S. Gottschalk, K. H. Wiesmuller, K. Ugurbil, M. E. Maier, J. Engelmann, *Bioconjugate Chem.* **2011**, *22*, 319 – 328.
[12] Z. Qian, P. G. Dougherty, D. Pei, *Chem. Commun.* **2015**, *51*, 2162 – 2165.
[13] S. M. Stanford, R. G. Panchal, L. M. Walker, D. J. Wu, M. D. Falk, S. Mitra, S. S. Damle, D. Ruble, T. Kaltcheva, S. Zhang, Z. Y. Zhang, S. Bavari, A. M. Barrios, N. Bottini, *Proc. Natl. Acad. Sci. USA* **2012**, *109*, 13972 – 13977.
[14] S. J. Riedl, Y. Shi, *Nat. Rev. Mol. Cell Biol.* **2004**, *5*, 897 – 907.
[15] D. J. Maly, L. Huang, J. A. Ellman, *ChemBioChem* **2002**, *3*, 16 – 37.
[16] N. A. Thornberry, T. A. Rano, E. P. Peterson, D. M. Rasper, T. Timkey, M. Garcia-Calvo, V. M. Houtzager, P. A. Nordstrom, S. Roy, J. P. Vaillancourt, K. T. Chapman, D. W. Nicholson, *J. Biol. Chem.* **1997**, *272*, 17907 – 17911.
[17] E. A. Slee, H. Zhu, S. C. Chow, M. MacFarlane, D. W. Nicholson, G. M. Cohen, *Biochem. J.* **1996**, *315*, 21 – 24.
[18] T. Pawson, P. Nash, *Science* **2003**, *300*, 445 – 452.
[19] H.-J. Lee, J. J. Zheng, *Cell Commun. Signaling* **2010**, *8*, 8.
[20] Z. Songyang, A. S. Fanning, C. Fu, J. Xu, S. M. Marfatia, A. H. Chishti, A. C. Crompton, A. C. Chan, J. M. Anderson, L. C. Cantley, *Science* **1997**, *275*, 73 – 77.
[21] M. Wolde, A. Fellows, J. Cheng, A. Kivenson, B. Coutermarsh, L. Talebian, K. Karlson, A. Piserchio, D. F. Mierke, B. A. Stanton, W. B. Guggino, D. R. Madden, *J. Biol. Chem.* **2007**, *282*, 8099 – 8109.
[22] S. H. Cheng, R. J. Gregory, J. Marshall, S. Paul, D. W. Souza, G. A. White, C. R. O'Riordan, A. E. Smith, *Cell* **1990**, *63*, 827 – 834.
[23] B.-S. Kerem, J. M. Rommens, J. A. Buchanan, D. Markiewicz, T. K. Cox, A. Chakravarti, M. Buchwald, L.-C. Tsui, *Science* **1989**, *245*, 1073 – 1080.
[24] P. R. Cushing, L. Vouilleme, M. Pellegrini, P. Boisguerin, D. R. Madden, *Angew. Chem. Int. Ed.* **2010**, *49*, 9907 – 9911; *Angew. Chem.* **2010**, *122*, 10103 – 10107.
[25] K. E. Roberts, P. R. Cushing, P. Boisguerin, D. R. Madden, B. R. Donald, *PLos Comput. Biol.* **2008**, *8*, e1002477.
[26] R. Kundu, P. R. Cushing, B. V. Popp, Y. Zhao, D. R. Madden, Z. T. Ball, *Angew. Chem. Int. Ed.* **2012**, *51*, 7217 – 7220; *Angew. Chem.* **2012**, *124*, 7329 – 7332.
[27] J. F. Amacher, P. R. Cushing, L. Brooks 3rd, P. Boisguerin, D. R. Madden, *Structure* **2014**, *22*, 82 – 93.
[28] E. Cormet-Boyaka, M. Jablonsky, A. P. Naren, P. L. Jackson, D. D. Muccio, K. L. Kirk, *Proc. Natl. Acad. Sci. USA* **2004**, *101*, 8221 – 8226.
[29] F. Van Goor, S. Hadida, P. D. J. Grootenhuis, B. Burton, J. H. Stack, K. S. Straley, C. J. Decker, M. Miller, J. McCartney, E. R. Olson, J. J. Wine, R. A. Frizzell, M. Ashlock, P. A. Negulescu, *Proc. Natl. Acad. Sci. USA* **2011**, *108*, 18843 – 18848.
[30] N. Pedemonte, G. L. Lukacs, K. Du, E. Caci, O. Zegarra-Moran, L. J. V. Galietta, A. S. Verkman, *J. Clin. Invest.* **2005**, *115*, 2564 – 2571.

Received: December 1, 2014
Revised: February 23, 2915
Published online: March 17, 2015

